ORNL/M-3253

ornl

OAK RIDGE NATIONAL LABORATORY

MARTIN MARIETTA

Thermal Resistance of Attic Looose-Fill Insulations Decreases Under Simulated Winter Conditions

R. S. Graves
K. E. Wilkes
D. L. McElroy

MANAGED BY
MARTIN MARIETTA ENERGY SYSTEMS, INC.
FOR THE UNITED STATES
DEPARTMENT OF ENERGY

ORNL/M-3253

Metals and Ceramics Division

THERMAL RESISTANCE OF ATTIC LOOSE-FILL INSULATIONS DECREASES UNDER SIMULATED WINTER CONDITIONS

R. S. Graves, K. E. Wilkes, D. L. McElroy

Date Published - May 1994

NOTICE: This document contains information of a preliminary nature. It is subject to revision or correction and therefore does not represent a final report.

Prepared for the
U. S. Department of Energy
Office of Buildings Energy Research

Prepared by
OAK RIDGE NATIONAL LABORATORY
Oak Ridge, Tennessee 37831
managed by
MARTIN MARIETTA ENERGY SYSTEMS, INC.
for the
U.S. DEPARTMENT OF ENERGY
under contract DE-AC05-84OR21400

)E F 1332.15
3-93)
mbines previous
rsion of DOE
1332.15 and .16.
other editions are
solete.

OMB Control No. 1910-1400
OMB Burden Disclosure Statement on reverse side

U. S. DEPARTMENT OF ENERGY
RECOMMENDATIONS FOR THE ANNOUNCEMENT AND DISTRIBUTION OF DEPARTMENT OF ENERGY (DOE) SCIENTIFIC AND TECHNICAL INFORMATION (STI)

(See instructions on reverse side. Use plain bond paper if additional space is needed for explanations.)

ART I *(DOE, DOE Contractors, Grantees, and Awardees complete)*

A. Product/Report Data

1. (Award) Contract No. DE-AC05-84OR21400

2. Title Thermal Resistance of Attic Loose-Fill Insulations Decreases Under Simulated Winter Conditions

3. Product/Report Description

☒ a. Report *(Complete all that apply)*

(1) ☒ Print ☐ Nonprint *(specify)*

(2) ☐ Quarterly ☐ Semiannual ☐ Annual ☐ Final

☒ Topical ☐ Phase I ☐ Phase II

☐ Other *(specify)*

Dates covered ______ thru ______

☐ b. Conference/Meeting/Presentation *(Complete all that apply)*

(1) ☐ Print ☐ Nonprint *(specify)*

☐ Published proceedings

☐ Other *(specify)*

(2) Conference Title *(no abbreviations)*

Location *(city/state/country)*

Date(s) *(m/d/y)* __/__/__ thru *(m/d/y)* __/__/__

Sponsor

☐ c. Software—Additional forms are required. Follow instructions on the back of this form.

☐ d. Other *(Provide complete description)*

B. Patent Information

Yes No

☐ ☒ Is any new equipment, process, or material disclosed? If yes, identify page numbers

☐ ☒ Has an invention disclosure been submitted? If yes, identify the disclosure number and to whom it was submitted. Disclosure number
Submitted to

☐ ☒ Are there patent-related objections to the release of this STI product? If so, state the objections.

C. Contact *(Person knowledgeable of content)*

Name

Phone

Position

Organization

PART II *(DOE/DOE Contractors complete/or as instructed by DOE contracting officer)*

A. DOE Identifiers

1. Product/Report Nos. ONRL/M-3253

2. Funding Office(s) *(NOTE: Essential data)* EC 21 01 00 0

B. Copies for Transmittal to AD-21 (OSTI)

(STI must be of sufficient quality for microfilming/copying.)

☐ 1. One for classified processing

☐ 2. ____ *(number)* for standard classified distribution

☒ 3. Two unclassified for processing

☐ 4. ____ *(number)* for program unclassified distribution

☒ 5. UC/C Category 369

☐ 6. Additional instructions/explanations

(Do not identify Sigma categories for Nuclear Weapons Data reports, and do not provide additional instructions that are inconsistent with C below.)

C. Recommendation *("X" at least one)*

☒ 1. Program/Standard Announcement/Distribution
(Available to U.S. and foreign public)

☐ 2. Classified *(Standard Announcement only)*

☐ 3. Special Handling *(Legal basis must be noted below.)*

☐ a. Unclassified Controlled Nuclear Information (UCNI)

☐ b. Export Control/ITAR/EAR

☐ c. Temporary hold pending patent review

☐ d. Translations of copyrighted material

☐ e. Small Business Innovation Research (SBIR)

☐ f. Commercializable information

☐ (1) Proprietary

☐ (2) Protected CRADA information
Release date __/__/__

☐ (3) Other *(explain)*

☐ 4. Program Directed Special Handling *(copy attached)*

D. Releasing Official

A. Patent Clearance *("X" one)*

☐ Has been submitted for DOE patent clearance

☒ DOE patent clearance has been granted

B. Released by

(Name) D.R. Hamrin

(Signature) D. R. Hamrin (KB)

(Phone) (615) 574-6752

(Date) May 31, 1994

TABLE OF CONTENTS

LIST OF FIGURES

LIST OF TABLES

THERMAL RESISTANCE OF ATTIC LOOSE-FILL INSULATIONS DECREASES UNDER SIMULATED WINTER CONDITIONS[1]

R. S. Graves, K. E. Wilkes, and D. L. McElroy

ABSTRACT

Two absolute techniques were used to measure the thermal resistance of attic loose-fill insulations: the Large Scale Climate Simulator (LSCS) and the Unguarded Thin-Heater Apparatus (UTHA). Two types of attic loose-fill insulations (unbonded and bonded/cubed) were tested under simulated winter conditions. To simulate winter conditions for an attic insulation, the specimens were tested with heat flow up, large temperature differences, and an air gap. The specimens were tested either with a constant mean temperature (30 or 21°C) and an increasing temperature difference or with a constant base temperature (21°C) and an increasing temperature difference (i.e., a decreasing mean temperature).

The UTHA test specimens had a nominal thickness of 0.2 m of loose-fill insulation. The LSCS test specimens had a nominal thickness of 0.3 m of loose-fill insulation contained in a 4.2 by 5 m attic test module with a gypsum board base. The module had a gabled attic with a 5 in 12 slope roof. The tests yielded the surface-to-surface thermal resistance, R, which includes the thermal resistance due to gypsum, insulation, and any wood joists. Tests with and without an air gap were conducted in the UTHA. Surface-to-surface thermal resistance results from the LSCS and the UTHA show similar trends for these two types of loose-fill insulation when tested under simulated winter conditions.

Tests with no air gap gave values of R that agreed with the bag label R-value for the insulations; R increased with lower mean temperatures. These no-gap values of R were 2 to 5% greater than the values of R obtained with an air gap for temperature differences of less than 22°C. For larger temperature differences R decreased, and at temperature differences of over 40°C, the R values were 50% less than those at small temperature differences. This phenomenon was observed on both types of fibrous glass loose-fill insulations: unbonded and bonded/cubed. The onset of the decrease in R for the bonded/cubed insulation occurs near a temperature difference of 25°C for a base temperature of 21°C. The temperature difference at which the R started to decrease obtained from the UTHA on specimens with R-values near 3.3 $m^2 \cdot K/W$ agreed with results from the LSCS on specimens with R-values near 5.3 $m^2 \cdot K/W$.

Air-flow permeabilities were measured with apparatus similar to that described in ASTM C 522. The air-flow permeabilities of the as-blown fiberglass specimens were in the range 20 to 80 x 10^{-9} m^2 and were inversely proportional to the density raised to about the third power. The shape of the thermal resistance-temperature difference curve is characteristic of heat transfer by natural convection. The onset of the decrease in thermal resistance is consistent with measured values of air-flow permeabilities and a critical Rayleigh number of 29 or less for an attic insulation with an open top.

---

[1]Research sponsored by the Office of Buildings Energy Research, U.S. Department of Energy, as part of the National Program for Building Thermal Envelope Systems and Materials, managed by Martin Marietta Energy Systems, Inc., under contract DE-ACO5-84-OR21400.

1. INTRODUCTION

Procedures to prepare a test specimen of a loose-fill insulation and to measure its thermal resistance (R-value) are described in ASTM C 687.(1) The test procedure for R-value allows hot-plate and hot-box techniques to be used, but states a preference for the heat-flow meter technique, ASTM C 518 (2), because it requires a shorter testing time and hence costs less. The testing technique described in ASTM C 687/C 518 uses heat flow up with flat plates contacting the upper and lower specimen surfaces (no air gap). The measured thermal resistance of the specimen obtained using flat plates contacting the specimen provides a needed market-place description of the material. Heat flow up provides a simulation of attic conditions in the winter. This is obtained by a warm lower plate and may induce convective effects since hot, low density air near the lower surface would have a tendency to rise through the insulation test specimen. The contacting upper plate does not simulate an open-top attic insulation installation. An open-top test with an air gap may enhance convection. Recent large-scale tests of some attic insulations that included open-tops, heat flow up, and a lower face temperature near 20°C, showed the thermal resistance to decrease by as much as a factor of two as the temperature on the upper side was decreased from 7°C to -28°C. The additional heat flow is due to natural convection of air through the insulation.(3-12) Tests at ORNL were conducted in the Large Scale Climate Simulator (LSCS) at the ORNL Building Envelope Research Center. The LSCS is expensive to operate. Thus, a demonstration of this phenomenon in the ORNL Unguarded Thin-Heater Apparatus (UTHA) using relatively small size test specimens could yield an economical means to simulate winter conditions for attic installations.

2. EQUIPMENT DESCRIPTION

2.1 LARGE SCALE CLIMATE SIMULATOR (LSCS)

Experiments were performed using an attic test module in the Large Scale Climate Simulator (LSCS) at the ORNL Roof Research Center.(13) The attic test module separated the upper climate chamber from the lower metering and guard chambers. The temperatures in the metering and guard chambers were both controlled at a constant level of 21°C, while the temperature in the climate chamber was controlled at various steady levels between 7°C and -28°C. The attic test module simulated a typical gabled attic residential construction. For most of the tests, a ventilation rate of about 0.5 $L/m^2{\cdot}s$ of attic floor was used. Primary instrumentation was four arrays of 21 thermocouples each, arranged midway between the joists to measure temperatures in the metering chamber air, at the bottom surface of the gypsum board, at the top surface of the insulation, and in the attic air 76 mm above the insulation. LSCS tests were run for about 24 hours. The average heat flow through the ceiling, and all temperatures averaged over the array for a particular surface yielded the surface-to-surface thermal resistance, R(SS):

$$R(SS) = A(T_b - T_t)/Q \qquad (1)$$

The resistance defined in Equation 1 includes resistances due to the gypsum board, insulation, and the wood joists. Specimens tested in the LSCS were blown using a Unisul Electric Volu-matic III Open Blow Machine.(14) The accuracy of the LSCS apparatus has been assessed by Wilkes and Childs (15) on two sets of panels of expanded polystyrene which show 95% reproducibility intervals of less than 2.6% and a bias of less than 4.3%.

2.2 THE UNGUARDED THIN-HEATER APPARATUS (UTHA)

The UTHA meets the requirements of ASTM C1114.(16) The apparatus is an absolute, longitudinal heat-flow method and consists of an unguarded, electrically-heated, flat, large-area Nichrome screen-wire heat source sandwiched between two horizontal layers of insulation with flat isothermal bounding surfaces. The heat source provides vertical heat flow in its central region across the subject insulation to two temperature-controlled, water-cooled, copper plates. The screen area is large (0.9 x 1.6 m) and is instrumented with 11 thermocouples for temperature measurement and voltage taps for power measurements. For two-sided heat flow, the thermal conductivity, k, is calculated for linear heat flow assuming half of the power generated flows through each layer,

$$k = I \times \Delta V \times L/(2 \times A_o \times \Delta T) \qquad (2)$$

For one-sided mode of operation, one plate is controlled to the temperature of the screen-wire heater, and the thermal conductivity is calculated from a correction for the small temperature mismatch between the screen and the guard plate. The reproducibility and repeatability of the k measurements have been determined to be 0.2%.(17, 18) Tests conducted in 1983 and 1990 on two standard reference materials (SRMs) from the National Institute of Standards and Technology are reported in Ref. 19 and show UTHA k values for the SRMs to be within the most probable uncertainty of 1.2%.

For tests in the UTHA, the loose-fill insulation test specimens were housed in a cavity, 0.216 x 0.89 x 1.27 m, built from 25.4 mm thick expanded polystyrene board on a 12 mm thick gypsum board. The loose-fill insulation test specimen was prepared using a Unisul Electric Volu-Matic III Open Blow Machine.(14) Empty frames, 76 mm x 0.89 m x 1.27 m, built from 25.4 mm thick expanded polystyrene boards could be placed on top of the test specimen frame to create a 76 mm or a 152 mm air space above the insulation specimen. A schematic drawing of this assembly is shown in Figure 1. Five Nichrome screen-wire pads, 30 x 30 mm, instrumented with Type E thermocouples were positioned with insulation sleeving at the upper surface of the loose-fill test specimen. This allowed R values as defined by Equation 1, to be obtained during each steady-state, one-sided, heat-flow test.

2.3 AIR FLOW PERMEABILITY APPARATUS

The air-flow permeability is defined by Darcy's law (12),

$$V = -\frac{K}{\mu}\frac{dP}{dx} \tag{3}$$

To calculate K from the experimental measurements, Darcy's law was integrated and rearranged to give

$$K = \frac{\mu}{A}\frac{L}{\Delta P/F} \tag{4}$$

Air-flow permeabilities were measured with the apparatus shown schematically in Figure 2, which follows the general principles outlined in ASTM Method C 522.(20,21) Insulation specimens were blown into wood boxes having lateral dimensions of about 610 by 610 mm.(14) Air from a cylinder of compressed air was passed through a Meriam laminar-flow element, then through a high-density fiberglass board that acted as a flow straightener, and finally through the specimen and into the surrounding atmosphere. The pressure drop through the laminar flow element was read using a Validyne differential pressure transducer, and was converted to a volumetric flow rate using the calibration supplied with the flow element. Since expansion of the high pressure air from the cylinder caused a cooling effect, the temperature of the air stream was measured to take into account the variation of air viscosity with temperature. The pressure drop across the specimen was measured with

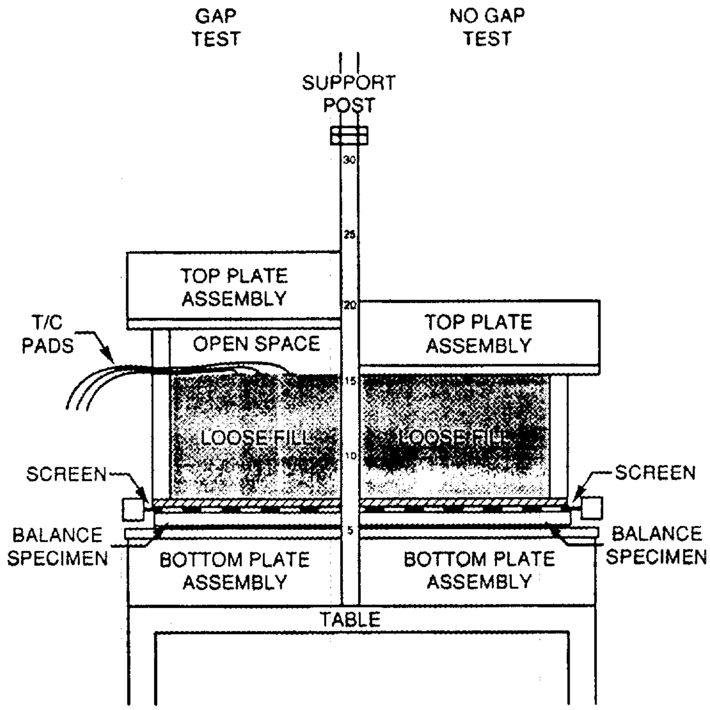

Fig. 1. Schematic drawing of loose-fill insulation specimen assembly used in the unguarded thin-heater apparatus.

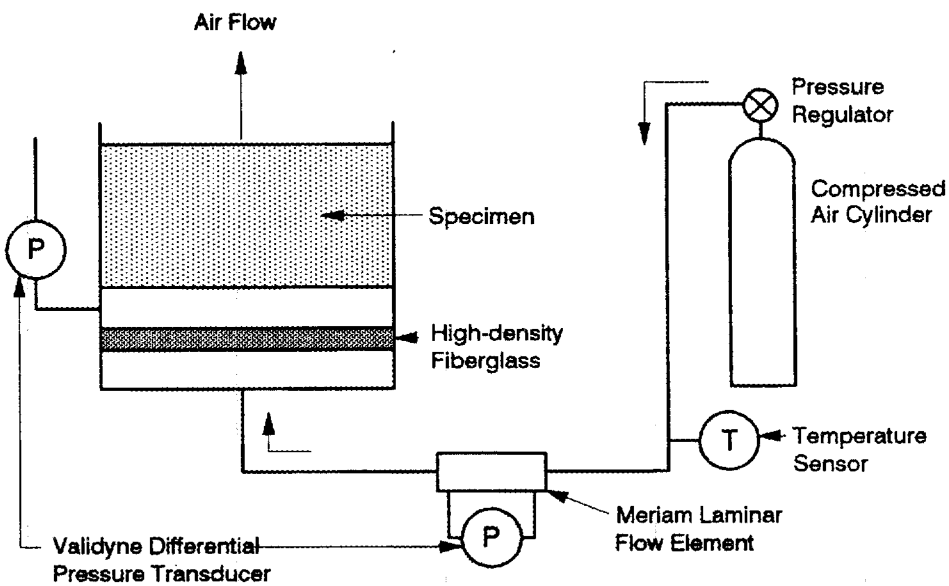

Fig. 2. Schematic of Air-Flow Permeability Apparatus.

a Validyne differential pressure transducer.

Measurements were made at six or more different flow rates between 0 and 1.1 liter per second, corresponding to velocities of 0 to 3 mm/s. Pressure differences across the specimen were 4 Pa or less. In all cases, a plot of ΔP versus F was a straight line, and a linear regression was used to obtain the ratio, $\Delta P/F$ for use in Equation 4. Coefficients of determination (r^2) were greater than 0.99 for most of the tests, but were as high as 0.9999 and as low as 0.87 for some of the tests.

3. TEST RESULTS

3.1 AIR-FLOW PERMEABILITY

Tables 1 and 2 list the air-flow permeabilities measured on specimens of bonded/cubed and unbonded loose-fill fiberglass. Figure 3 shows permeability versus density, along with curves obtained from linear regressions of log K versus log ρ. Equations 5 and 6 are the equations for the bonded/cubed and unbonded insulations, respectively:

$$K = 1.6184\ X\ 10^{-5}\ \rho^{-2.82} \tag{5}$$

$$K = 6.4359\ X\ 10^{-5}\ \rho^{-3.41} \tag{6}$$

Coefficients of determination, as obtained from the linear regressions of log K versus log ρ, are 0.810 and 0.856 for Equations 5 and 6, respectively.

3.2 THERMAL TEST RESULTS FROM THE LSCS

Characteristics of attic loose-fill insulations tested in the LSCS are given in Table 3. Two specimens of unbonded (U) and one specimen of bonded/cubed (BC) fiberglass insulation were tested at thicknesses of 0.33 to 0.38 m. For specimen U-1, the average thickness and mass of the insulation from the central metering area were determined following the thermal tests. For the other two specimens, additional tests (not reported here) only allowed the thickness and mass values to be estimated.

Both specimens of the unbonded material were tested under thermal conditions that simulate those encountered in a typical attic: the air below the ceiling was maintained near 21°C for all tests, while the temperature in the climate chamber was maintained at various steady temperatures to simulate outdoor winter temperature conditions between 7°C and -28°C. This set of conditions is

Table 1. Air-flow permeability of bonded/cubed loose-fill fiberglass insulation

Specimen	Thickness, mm	Density, kg/m^3	Permeability, m^2 X 10^9
1	412	8.92	28.5
2	404	8.81	28.7
3	405	8.92	27.3
4	405	9.52	23.0
5	216	8.19	54.8
6	206	7.96	59.7
7	196	8.10	63.4
8	202	8.01	74.7
1	188	6.76	62.2
1	224	10.7	19.7
2	138	5.97	80.1
2	266	10.2	21.5
3	187	6.71	68.9
3	218	10.8	18.0

Table 2. Air-flow permeability of unbonded loose-fill fiberglass insulation

Specimen	Thickness, mm	Density, kg/m^3	Permeability, m^2 X 10^9
1	308	8.29	54.6
2	320	8.22	44.0
3	307	8.22	49.5
4	299	8.30	45.9
5	219	7.74	68.1
6	216	7.87	68.9
7	211	7.56	61.0
8	234	7.14	78.5
9	226	7.60	72.9
1	272	9.38	35.5
1	227	11.2	16.6
2	277	9.50	28.0
2	238	11.1	15.0
3	46	6.07	61.1
3	84	7.56	104
3	63	8.14	37.0
3	114	9.62	38.7
4	56	5.71	245
4	77	7.52	55.0
4	76	9.16	33.8
4	90	9.85	34.2
1	92	11.4	11.9
1	135	11.2	22.7
2	108	11.4	12.0
2	130	10.8	19.0

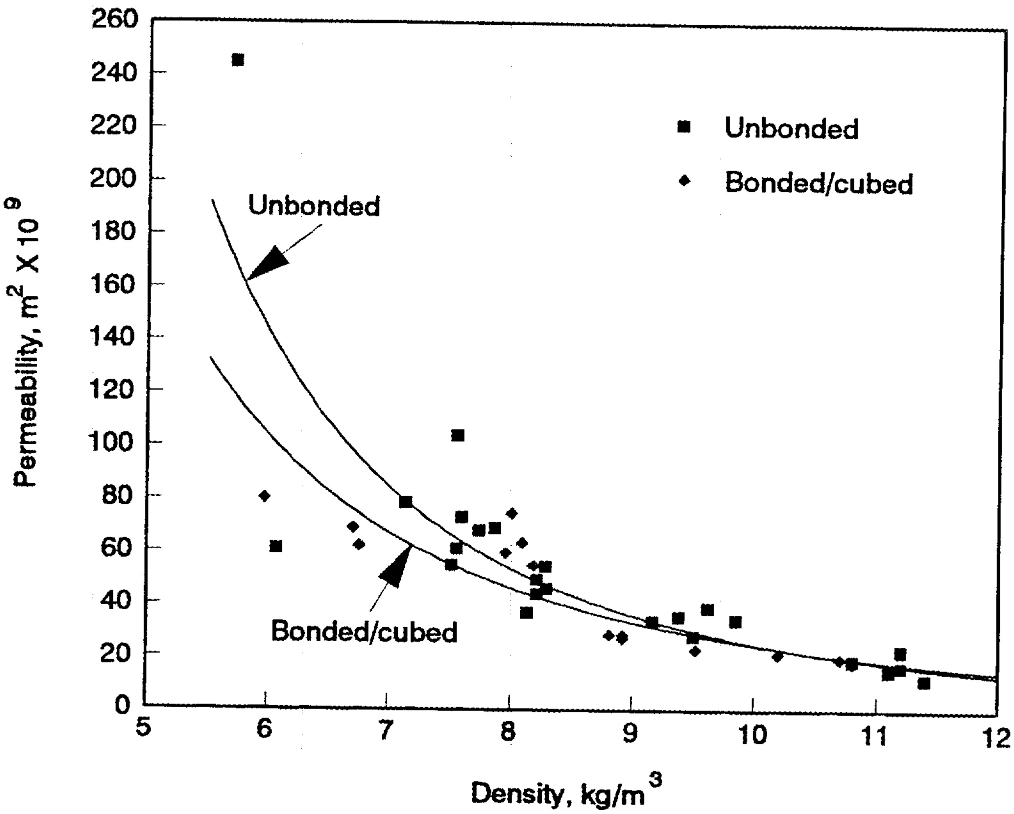

Fig. 3. Permeability of loose-fill fiberglass.

Table 3. Properties of attic loose-fill insulation specimens tested in the UTHA and the LSCS.

A. Tested in the Unguarded Thin Heater Apparatus (UTHA)			
Specimen	Insulation Thickness	Density	Weight
	m	kg/m^3	kg/m^2
Unbonded			
U-NJ: Air Gap	0.23 (a)	7.82	2.39
No Gap	0.22 (b)	8.14	1.76
U-J: Air Gap	0.21 (a)	9.29	1.95
No Gap	0.22 (b)	9.13	1.94
Bonded/Cubed			
BC-J	0.22	7.52	1.63
BC-NJ	0.21	8.43	1.78
B. Tested in the Large Scale Climate Simulator (LSCS)			
Unbonded			
U-1	0.34	8.7	3
U-2	0.33	7-9.5	2.3-3.2
Bonded/Cubed			
BC-1	0.38(c)	7.2(c)	2.7(c)

a. Pin gage thickness.
b. From plate to plate thickness.
c. Estimated

referred to as "base". The bonded/cubed material was also measured under a second set of conditions wherein the mean temperature of the insulation was maintained constant near 22°C by varying the temperatures in both the climate and metering chambers. This set of conditions is referred to as "mean".

Results of tests in the LSCS are given in Table 4 and are plotted in Figure 4. For both unbonded specimens, (U-1 and U-2), the resistance at temperature differences of 18 K or less averaged about 5.4 $m^2 \cdot K/W$, increased as the mean temperature increased under the "base" conditions. As the temperature difference increased above 18 K, the resistance started to decrease, and when the temperature difference reached about 40 K, the resistance had decreased by about 45 percent.

For the bonded/cubed insulation under "base" conditions, the resistance started at 5.7 $m^2 \cdot K/W$ at a temperature difference of 14 K, rose to 6.1 $m^2 \cdot K/W$ at a difference of 24 K, and then decreased with larger temperature differences, until at a temperature difference of 45 K the resistance had decreased by about 47 percent. Under "mean" conditions, the resistance was approximately constant at 5.6 $m^2 \cdot K/W$ at temperature differences of 29 K and smaller; above 29 K, the resistance decreased until at a temperature difference of 47 K it had decreased by about 32 percent. As shown in Figure 4, the intersection of a horizontal line at 5.6 $m^2 \cdot K/W$ with a straight line through the higher temperature difference data points occurs at a temperature difference of 31 K.

The shape of the resistance-temperature difference curves is characteristic of heat transfer by natural convection. For a horizontal porous medium heated from below, no convection is expected until a certain critical temperature difference is reached, after which the resistance starts to decrease with increasing temperature difference. The hypothesis of the occurrence of natural convection has been confirmed through infrared images of the top of the insulation (5). These revealed a hexagonal pattern that is also characteristic of some natural convection configurations, with cold dense air from the attic flowing down into the insulation at the cores of the hexagons, being heated from below, and the warmer, less dense air flowing up out of the insulation at the perimeters of the hexagons.

Theory (12) shows that the onset of convection in a horizontal porous medium is governed by the dimensionless Rayleigh number, Ra, which is defined as:

$$Ra = \frac{g\beta\rho C_p LK \, \Delta T}{\nu k} \qquad (7)$$

Table 4. Surface-to-surface thermal resistances of ceilings insulated with low-density loose-fill fiberglass determined in the LSCS

A. Unbonded, Constant Base, Specimen 1

SI Units		
T_b	T_t	R
20.7	8.1	5.25
20.4	1.9	5.37
20.2	-3.9	5.00
20.1	-9.7	4.01
19.9	-14.9	3.48
19.5	-20.4	2.94

B. Unbonded, Constant Base, Specimen 2

SI Units		
T_b	T_t	R
20.9	8.5	5.39
20.3	2.2	5.61
20.2	-9.0	4.15
19.4	-20.5	3.00

Note: T_b = temperature of bottom of gypsum board ceiling, °C.
T_t = temperature of bottom of gypsum board ceiling, °C.
R = thermal resistance between bottom of gypsum board and top of insulation system, $m^2 \cdot K/W$.

Table 4. Surface-to-surface thermal resistances of ceilings insulated with low-density loose-fill fiberglass determined in the LSCS (cont.)

C. Bonded/Cubed, Constant Base

SI Units		
T_b	T_t	R
20.5	6.0	5.71
20.4	1.1	6.06
20.3	-3.6	6.11
20.2	-7.7	5.45
20.1	-11.9	4.59
19.9	-16.3	4.15
19.5	-21.0	3.59
19.2	-26.1	3.21

D. Bonded/Cubed, Constant Mean

SI Units		
T_b	T_t	R
33.2	10.3	5.52
35.9	7.1	5.71
38.6	5.1	5.38
41.3	3.0	4.85
43.9	1.2	4.32
46.5	-0.7	3.79

Note: T_b = temperature of bottom of gypsum board ceiling, °C.
T_t = temperature of bottom of gypsum board ceiling, °C.
R = thermal resistance between bottom of gypsum board and top of insulation system, $m^2 \cdot K/W$.

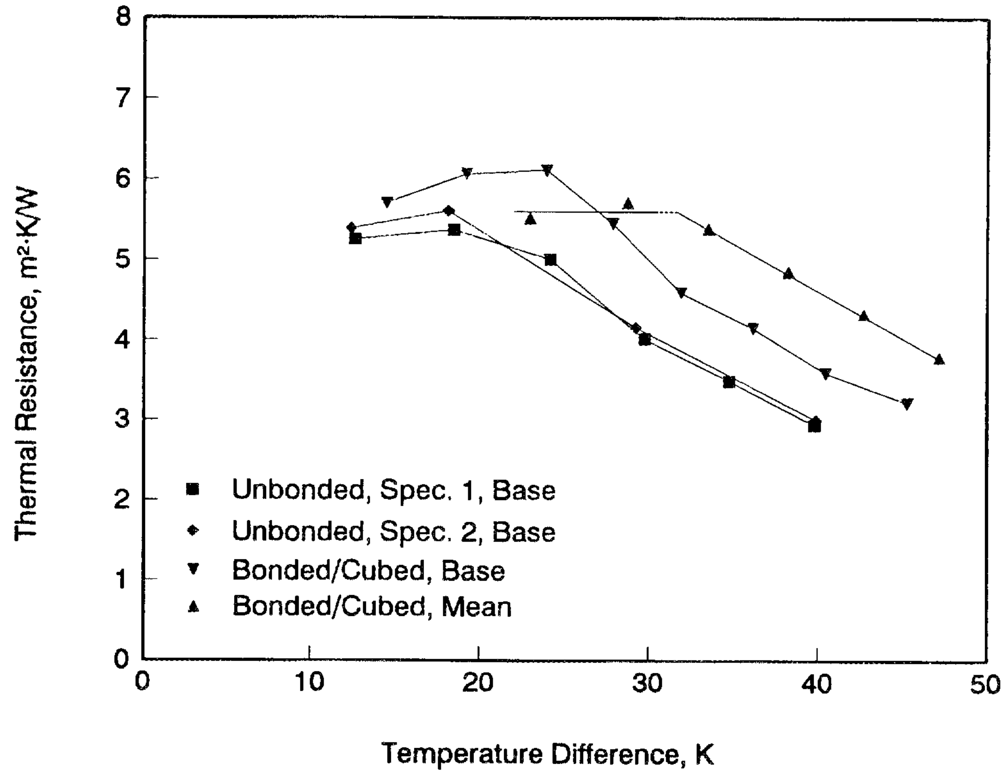

Fig. 4. Thermal Resistance of ceilings insulated with unbonded and bonded/cubed low-density loose-fill fiberglass as determined in the LSCS. The ordinate is the surface-to-surface thermal resistance between the bottom of the gypsum board and the top of the insulation system, and the abscissa is the temperature difference between these two locations.

The theories [2] also predict that the critical Rayleigh number, Rac, depends upon the thermal and mechanical boundary conditions imposed on the top and bottom surfaces of the insulation. For the configuration of attic insulation, with an open top surface, the Rac should be 27.1 or less.

The calculated Rac for unbonded specimen U-1 is 12, while that for unbonded specimen U-2 is 9 to 26 (depending upon which value of density, and hence, permeability is used). For the bonded/cubed insulation, for which the density was estimated, the Rac is calculated to be 28 for the "base" conditions. Using a critical temperature difference of 31 K for the "mean" condition, the Rac is 29. While there is uncertainty in these Rac values (mainly from the uncertainty in the permeability), they all fall within the range of 10 to 30 that has been observed in other experiments.(3, 10) In addition, Rac values for the "base" and "mean" conditions for the bonded/cubed fiberglass insulation are nearly identical, showing that the effects of differing mean temperatures can be accurately accounted for (note, the ratio of the critical Rayleigh numbers for these two conditions is not influenced by any uncertainty in the permeability).

3.3 THERMAL TEST RESULTS FROM THE UTHA

Characteristics of the loose-fill insulations tested in the UTHA are given in Table 3. Unbonded (U) and bonded/cubed (BC) loose-fill fiberglass insulations were tested in the UTHA as specimens with wood joists on 0.61 m centers (U-J and BC-J) and without joists (U-NJ and BC-NJ). The UTHA specimens were nominally 0.22 m thick and had densities between 7.5 and 9.3 kg/m^3.

Table 5 lists the thermal tests conducted in the UTHA on the unbonded and bonded test specimens. For example, the five tests on the unbonded, no joists specimen were conducted with air gaps of 76, 152, and 0 mm and at a mean nominal temperatures of 21 and 30°C. Tests were conducted on the unbonded, joist specimen and the bonded/cubed joist specimen with a base (gypsum) temperature of 21°C and a range of temperature differences (see asterisk, Table 5). The air gap tests of zero mm spacing correspond to the top plate contacting the upper surface of the insulation, which is the usual C 687 procedure for thermal testing of insulation. The surface-to-surface thermal resistance data for the UTHA specimens are tabulated in Tables 6, 7, and 8.

---

[2] It should be noted that the temperature difference used to define the Rayleigh number is not exactly equal to the surface-to-surface temperature difference used to define the thermal resistance. However, since the thermal resistance of the gypsum board (about 0.08 m^2K/W) is much smaller than the thermal resistance of the insulation in the absence of convection (about 3.5 to 7 m^2K/W), the difference between these two ΔTs is only about 1% to 2% and is, therefore, ignored in the discussion of the onset of convection.

Table 5. Air gap size and system temperatures for unbonded and bonded/cubed specimens tested in the UTHA.

Specimen Test		Air Thickness (mm)	Mean Temperature, (°C)	Table (Data Points)
Unbonded, No Joists U-NJ	Test 1	76	29.4	6 (7)
	2	152	30	6 (7)
	3	152	21	6 (4)
	4	0	29	6 (3)
	5	0	21	6 (1)
Unbonded, Joists U-J	1	152	29	7 (8)
	2	152	21	7 (7)
	3	152	21*	7 (4)
	4	0	30	7 (1)
	5	0	21	7 (1)
Bonded/Cubed-No Joists BC-NJ	1	152	22	8 (4)
	2	0	22	8 (2)
Bonded/Cubed, Joists BC-J	1	152	22	8 (5)
	2	152	21	8 (6)
	3	0	22	8 (2)

*Base temperature was 21°C.

Figure 5 shows the results of tests on the unbonded, no-joists specimen with a mean temperature of 30°C, and air gaps of 0, 76, and 152 mm. With no air gap, the resistance is 3.18 $m^2 \cdot K/W$ and nearly independent of temperature difference. With either air gap, the thermal resistance is near the value of 3.18 $m^2 \cdot K/W$ for temperature differences of 40 K or less. For larger temperature differences, the thermal resistance decreases with increasing temperature difference, until at the largest temperature difference of 55 K, the thermal resistance has decreased by about 20 percent. The curves for the 76 and 152 mm thick air gaps are very similar, but differ markedly from that for no air gap for temperature differences greater than 40 K. Because of the similarity of results with the two sizes of air gap, only the larger air gap was used for the remaining experiments. Using a critical temperature difference of 39.8 K, a Rac of 17.2 is calculated for the cases with air gaps. This is somewhat larger than the Rac of 12 calculated for the unbonded test in the LSCS. Theory shows that the addition of a solid plate on top of the insulation should increase the critical Rayleigh number by 46 percent. Hence the Rac for the no air gap case would be expected to be 25.1. This corresponds to a temperature difference of 58 K, which is beyond the range measured. Hence the difference in Rac between the case with no air gap and those with air gaps provides an explanation for the difference in curves of resistance versus temperature difference.

Figure 6 shows the results for the unbonded, no joists specimen with a 152 mm air gap and mean temperatures of 21°C and 30°C (Tests 2 and 3). At small temperature differences, a decrease in mean temperature from 30°C to 21°C results in a 5 percent increase in resistance. However, the decrease in mean temperature results in a smaller critical temperature difference so that the curves cross each other. Using the Rac of 17.2 calculated for the 30°C case, the critical temperature difference for the 21°C case would be expected to be 33.8 K, which agrees well with the experimental curve. For the unbonded insulation, R(SS) with no air gap at 21°C is 3.48 m^2K/W (Test 5), but R(SS) with an air gap is 5% less, 3.32 m^2K/W (Test 3).

Results for unbonded specimens with and without joists at a mean temperature of 21°C and with a 152 mm air gap are shown in Figure 7. Based on numerical calculations (11), it was expected that the joists would provide warm spots that would trigger convection at smaller temperature differences than in their absence. This expectation was not borne out by experiment, as these curves show. However, a direct comparison of these two sets of data to detect differences due to the joists is complicated by a difference in density of the insulation. The specimen with joists had a density about 19 percent larger than the one with no joists. Also the unbonded insulation with joists had an R with no air gap (Test 5) at 21°C that is 4% less than R with an air gap (Test 2). Using Equation

Table 6. Surface-to-surface thermal resistances of UTHA specimens of unbonded, loose-fill insulation with no joists.

Test 1 (7)		
T_b (°C)	T_t (°C)	R ($m^2 \cdot K/W$)
33.4	27.0	3.16
34.7	24.3	3.18
40.7	19.3	3.14
45.9	14.4	3.14
50.4	10.6	3.13
53.9	7.1	2.89
57.9	3.0	2.58
Test 2 (7)		
34.7	24.3	3.13
40.8	19.3	3.15
40.9	19.3	3.16
45.8	14.3	3.10
50.1	10.6	3.05
54.3	7.1	2.94
57.6	3.1	2.52
Test 3 (4)		
27.1	16.1	3.30
32.5	11.0	3.34
37.8	6.1	3.22
45.8	-1.3	2.68
Test 4 (3)		
34.7	24.1	3.15
46.0	13.7	3.20
57.8	1.7	3.18
Test 5 (1)		
37.5	5.3	3.48

Table 7. Surface-to-surface thermal resistance of UTHA specimens of unbonded, loose-fill insulation with joists.

Test 1 (8)		
T_b (°C)	T_t (°C)	R ($m^2 \cdot K/W$)
49.4	10.2	3.20
54.8	6.1	3.13
58.7	2.1	3.03
41.1	19.0	3.32
33.3	23.9	3.17
33.4	23.9	3.21
41.0	19.0	3.28
58.9	2.1	3.02
Test 2 (7)		
27.4	16.0	3.59
31.8	10.3	3.46
38.0	5.8	3.40
46.2	-2.0	3.29
27.5	16.0	3.64
29.4	13.2	3.48
24.8	19.2	3.65
Test 3 (4) Base at 21 °C		
21.0	10.4	3.66
21.2	5.7	3.75
21.2	0.8	3.73
21.0	-5.0	3.71
Test 4 (1)		
46.0	13.6	3.30
Test 5 (1)		
37.5	5.1	3.59

Table 8. Surface-to-surface thermal resistance of UTHA specimens of bonded/cubed insulation with and without joists.

Test 1 (4) Bonded/Cubed, No Joists		
T_b (°C)	T_t (°C)	R ($m^2 \cdot K/W$)
27.2	16.1	3.29
31.7	10.4	3.25
46.3	-1.6	2.77
38.6	5.8	3.23
Test 2 (2) Bonded/Cubed, No Joists		
30.6	13.5	3.34
37.9	5.3	3.35
Test 1 (5) Bonded/Cubed, Joists		
27.2	16.1	3.31
31.7	10.5	3.24
38.5	6.1	3.20
45.5	-1.0	2.70
26.2	19.3	3.16
Test 2 (6) Base of 21°C (70°F) Bonded/Cubed, Joists		
21.2	15.7	3.35
22.3	10.9	3.39
21.0	5.8	3.44
21.3	1.0	3.48
21.4	-4.9	3.45
21.4	-8.1	3.41
Test 3 (2) Bonded/Cubed, Joists		
37.7	5.3	3.28
30.5	13.6	3.31

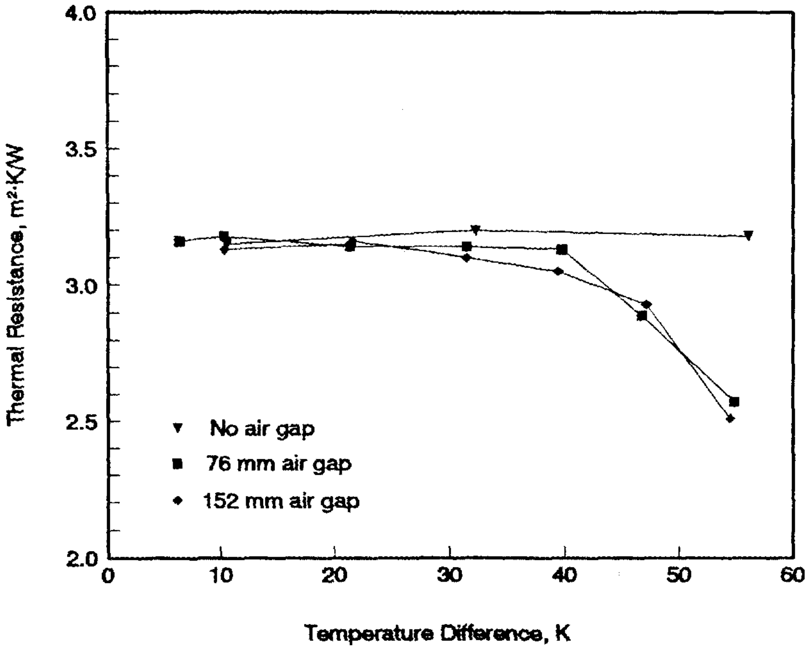

Fig. 5. Thermal Resistance of the unbonded, no joist specimen of low-density loose-fill fiberglass as a function of the size of the air gap as determined in the UTHA. The ordinate is the surface-to-surface thermal resistance between the bottom of the gypsum board and the top of the insulation system, and the abscissa is the temperature difference between these two locations.

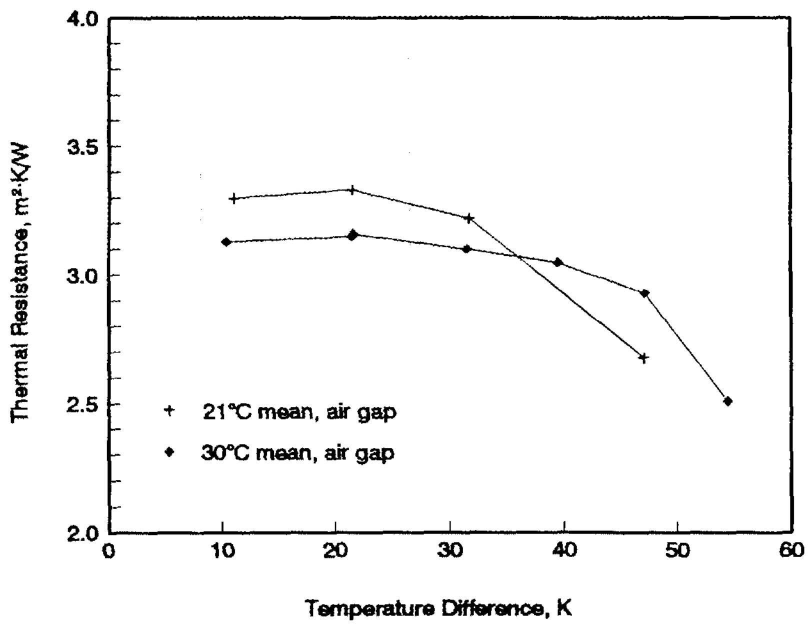

Fig. 6. Thermal Resistance of the unbonded, no joist specimen of low-density loose-fill fiberglass as a function of mean temperature as determined in the UTHA. The ordinate is the surface-to-surface thermal resistance between the bottom of the gypsum board and the top of the insulation system, and the abscissa is the temperature difference between these two locations.

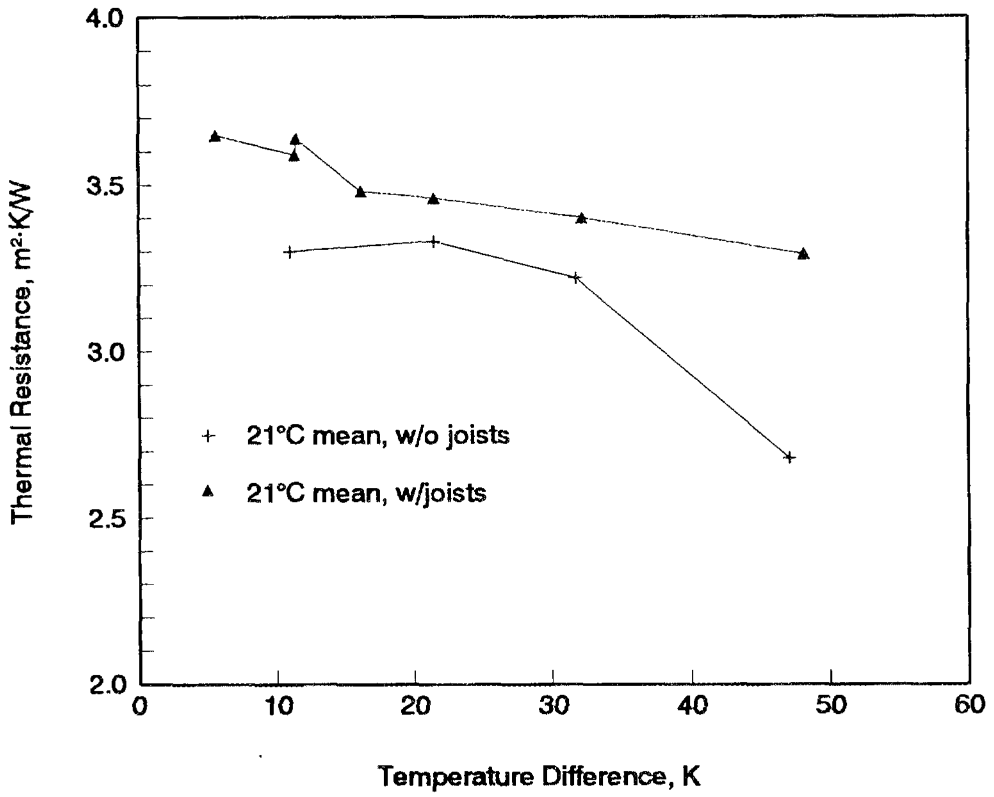

Fig. 7. Thermal Resistance of the unbonded, with and without joist specimens of low-density loose-fill fiberglass at a mean temperature of 21°C as determined in the UTHA. The ordinate is the surface-to-surface thermal resistance between the bottom of the gypsum board and the top of the insulation system, and the abscissa is the temperature difference between these two locations.

6, the air-flow permeability of the specimen with joists is expected to be 79 percent lower than the other. Hence with a Rac of 17.2, the critical temperature difference for the specimen with studs would be expected to be 61 K for 21°C mean and 71 K for the 30°C mean, both of which are beyond the range of the experiment. The fact that the resistance does decrease slightly over the temperature difference range measured may be an indication that the joists are causing a small amount of convection to occur even though the Rayleigh number is lower than the critical value.

A comparison of results with the "base" and "mean" conditions is given in Figure 8 for the unbonded specimen with joists and with an air gap of 152 mm. With the "base" conditions, the mean temperature varies from 15.7°C to 8.0°C as the temperature difference is increased. If no convection were present, this decrease in mean temperature would be expected to cause an increase in resistance. Even though Rayleigh numbers are less than 10 for the "base" measurements, the resistance first rises and then falls as the temperature difference is increased. Again, the slight falloff in resistance may be an indication of a small amount of convection caused by the joists even though the Rayleigh number is much below the critical value.

A composite of the data on bonded/cubed insulation in the UTHA is shown in Figure 9. All data were taken either with a 21°C mean or a 21°C base temperature. Either with or without joists, the resistance with constant mean temperature is essentially independent of temperature difference below about 32 K. For the bonded/cubed insulation R with no air gap was 2% greater than R with an air gap. At temperature differences greater than 32 K, the resistance decreases, with the decrease being larger for the case with joists. Critical Rayleigh numbers for the cases without and with joists are calculated to be 11.4 and 15.3, respectively. For the measurements with constant base temperature, the resistance increased as the temperature difference was increased from 6 K to 20 K and then started to decrease. Using the critical Rayleigh number of 15.3, the critical temperature difference for the "base" case would be expected to be about 26 K, which is in fairly good agreement with the experimental data. Critical Rayleigh numbers of 11 to 15 for the UTHA experiments are less than the value of 28 calculated for the LSCS tests on the same material. It is suspected that the estimates of density in the LSCS tests are too low.

3.4 COMPARISON OF TEST RESULTS FROM THE LSCS AND THE UTHA

Apparent thermal conductivities for the insulation may be calculated from the thermal resistance data that are considered not to be influenced by convection. Apparent thermal conductivity values for the insulation were calculated using an average of the ASHRAE parallel path

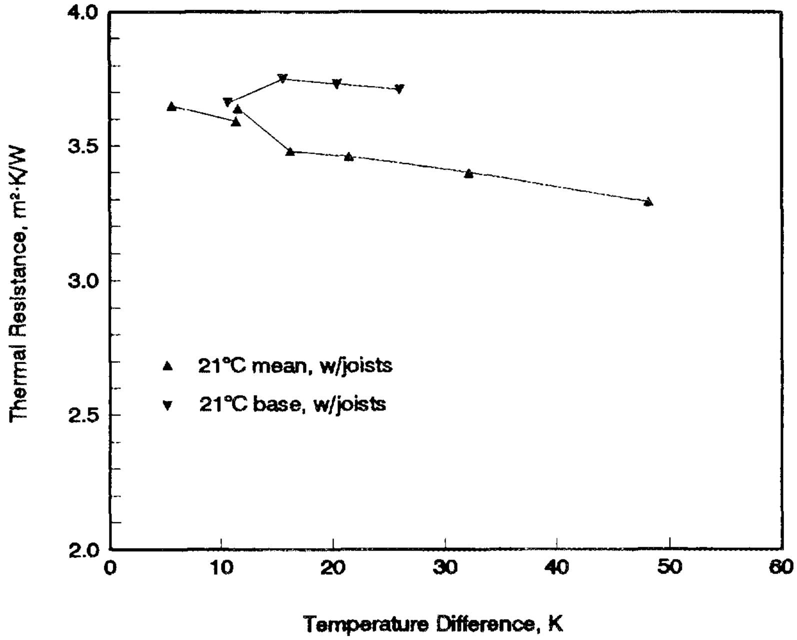

Fig. 8. Thermal Resistance of the unbonded, specimens of low-density loose-fill fiberglass at base and mean conditions as determined in the UTHA. The ordinate is the surface-to-surface thermal resistance between the bottom of the gypsum board and the top of the insulation system, and the abscissa is the temperature difference between these two locations.

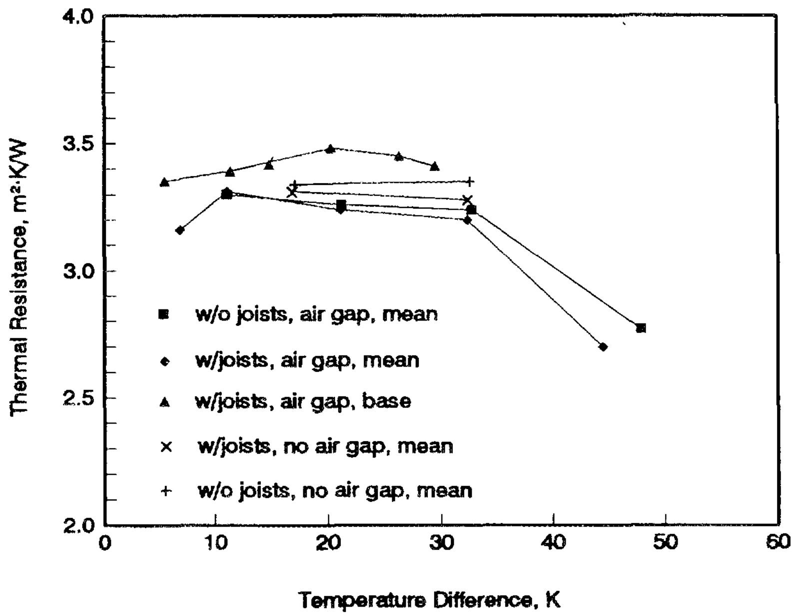

Fig. 9. Thermal Resistance of the bonded/cubed specimens of low-density loose-fill fiberglass as determined in the UTHA. The ordinate is the surface-to-surface thermal resistance between the bottom of the gypsum board and the top of the insulation system, and the abscissa is the temperature difference between these two locations.

and series-parallel methods.(22) These calculations assumed the thermal conductivities of wood and gypsum board to be 0.115 and 0.160 W/m·K, respectively.(22) Figure 10 shows the apparent thermal conductivity as a function of T^3/ρ, where T is the mean absolute temperature. In general, for low-density insulations, the thermal conductivity tends to vary linearly with T^3/ρ, with the values for the bonded/cubed material falling somewhat below those for the unbonded material. From this plot, it is seen that the thermal conductivities derived from the LSCS and the UTHA are in good agreement. By pooling the data from all the tests, the thermal conductivity may be represented by

$$k = 0.003393 + 7.586 \, X \, 10^{-5} \, T + 1.281 \, X \, 10^{-8} \, \frac{T^3}{\rho} \tag{8}$$

where the first two terms represent the thermal conductivity of air (23) and are independent of density. The third term represents the radiative contribution for the loose-fill insulation obtained from regression analysis of k without the thermal conductivity of air.

Another direct comparison between results from the LSCS and the UTHA can be obtained by examining dimensionless quantities. The Rayleigh number, defined in Equation 7, is a dimensionless number which accounts for differences in mean temperature, temperature difference, air-flow permeability, thickness, and apparent thermal conductivity. Correlations of convection data usually use the Nusselt number for the other dimensionless quantity, which is defined as the ratio of heat flow with convection to that without convection. Since our focus is on thermal resistance, we use a quantity that is essentially the inverse of the Nusselt: the ratio of the thermal resistance, R, divided by the thermal resistance at small Rayleigh numbers, Ro.

Dimensionless resistance ratios and Rayleigh numbers for the unbonded material are shown in Figure 11. This plot shows that the LSCS data are in good agreement with the UTHA data taken with an air gap over the insulation. For these tests, R/Ro is close to one for small Ra and then decreases when Ra exceeds about 12 to 18. However, for the UTHA tests with no air gap, R/Ro remains close to one for larger Ra. Theories for porous media with no gradients in air-flow permeability predict that the critical Rayleigh number is $4\pi^2$ when the porous medium is bounded by isothermal, impermeable surfaces on the top and bottom, and is 27.1 when the top surface is open.(12) When there is a large variation in air-flow permeability through the thickness of the porous medium (such as was observed for these materials), theory indicates that the critical Rayleigh number is reduced from the $4\pi^2$ value to about 28. It is speculated that a variable permeability may

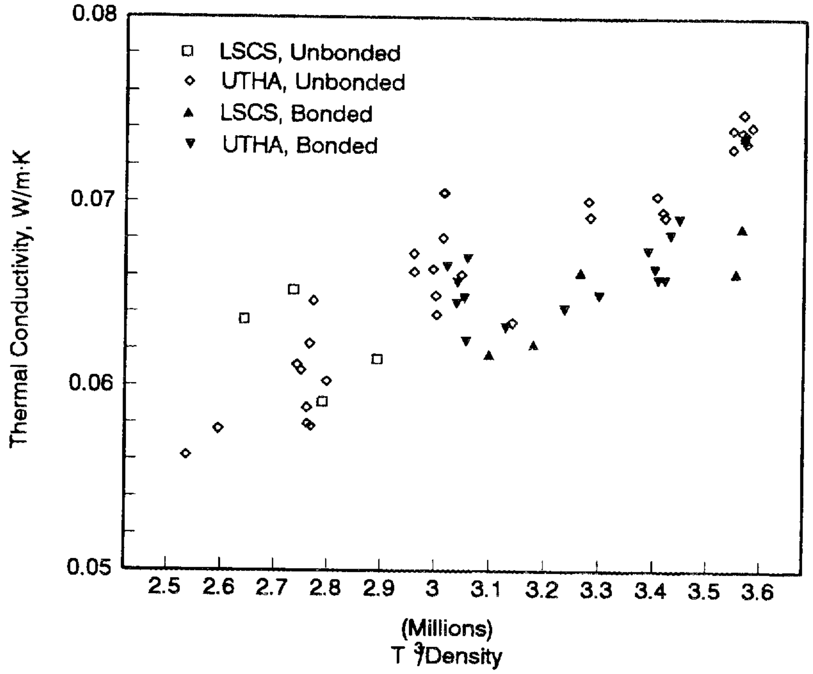

Fig. 10. Apparent thermal conductivity of the loose-fill insulations as a function of T^3/ρ for the LSCS and UTHA for data without convection effects.

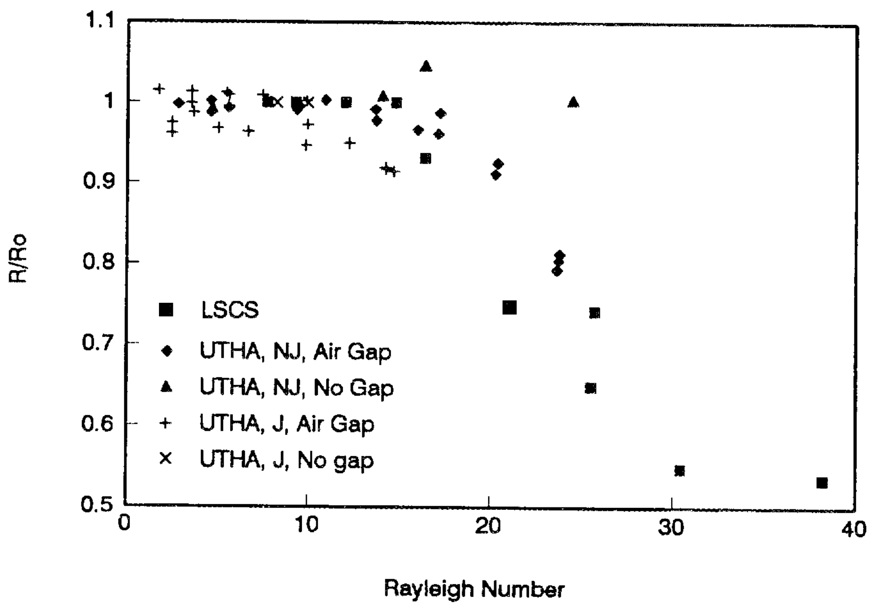

Fig. 11. Normalized thermal resistance as a function of the Rayleigh number for the unbonded insulation. Resistance values are normalized by dividing them by the resistance at small Rayleigh numbers.

also reduce the 27.1 value by the same percentage, to a value of about 19. Critical Rayleigh numbers of 19 and 28 for the open and closed tops are consistent with the data in Figure 11.

Figure 12 shows R/Ro versus Ra for the bonded/cubed material. Here, the agreement between the UTHA and the LSCS data is not as good. As was mentioned above, the density of the LSCS specimen was not directly determined, and the uncertainty in density is thought to be the cause of the differences between the data from the two apparatuses. Because of the strong variation of air-flow permeability with density, an error in the density will be magnified into a larger error in Ra. For example, if the density were 15 percent larger, the Ra values would all be reduced by 33 percent, bringing the results of the two apparatuses into good agreement. The UTHA data for the bonded/cubed material are in good agreement with those obtained on the unbonded material. It should also be noted that the values for the LSCS data in Figure 12 include both the data obtained under the "base" conditions as well as the "mean" conditions. By plotting dimensionless values, the data obtained under these two conditions fall on the same curve.

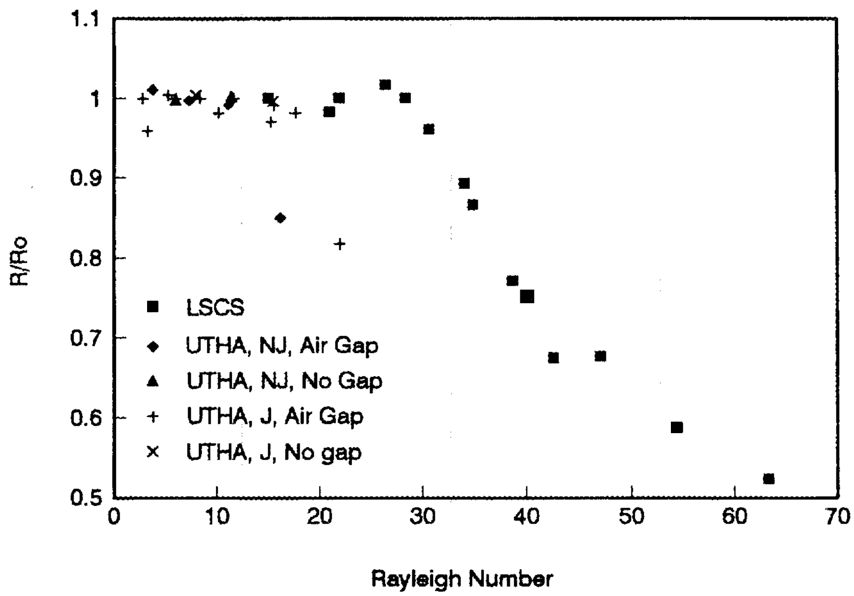

Fig. 12. Normalized thermal resistance as a function of the Rayleigh number for the bonded/cubed insulation. Resistance values are normalized by dividing them by the resistance at small Rayleigh numbers.

4. ACKNOWLEDGEMENTS

Dr. D. W. Yarbrough, Dr. Thomas G. Kollie, and Mr. Andre O. Desjarlais of ORNL are thanked for reviewing this manuscript. The authors thank Ms. Linda Parker for preparing the manuscript.

5. REFERENCES

1. "Standard Practice for Determination of Thermal Resistance of Loose-fill Building Insulation," ASTM C 687-91, pp. 330-338 in 1992 Annual Book of ASTM Standards, Vol. 04.06, American Society for Testing and Materials, Philadelphia, 1992.

2. "Standard Test Method for Steady-state Heat Flux Measurements and Thermal Transmission Properties by Means of the Heat Flow Meter Apparatus", ASTM C 518-91, pp. 153-164 in 1992 Annual Book of ASTM Standards, Vol. 04.06, American Society for Testing and Materials, Philadelphia, 1992.

3. K. E. Wilkes and J. R. Rucker, "Thermal Performance of Residential Attic Insulation," Energy and Buildings, Vol. 5, pp. 263-277, 1983.

4. R. W. Besant and E. Miller, "Thermal Resistance of Loose-Fill Fiberglass Insulations in Spaces Heated from Below," Proceedings, ASHRAE/DOE Conference on Thermal Performance of the Exterior Envelopes of Buildings II, ASHRAE 38, pp. 720-733, 1983.

5. K. E. Wilkes, R. L. Wendt, A. Delmas, and P. W. Childs, "Attic Testing at the Roof Research Center-Initial Results," pp. 391-400, 1991 International Symposium on Roofing Technology, 1991.

6. K. E. Wilkes, R. L. Wendt, A. Delmas, and P. W. Childs, "Thermal Performance of One Loose-Fill Fiberglass Attic Insulation," pp. 275-291 in Insulation Materials: Testing and Applications, 2nd Volume, ASTM STP 1116, R. S. Graves and D. C. Wysocki, Eds., American Society for Testing and Materials, Philadelphia, 1991.

7. William B. Rose and David J. McCaa, "The Effect of Natural Convective Air Flows in Residential Attics on Ceiling Insulating Materials," pp. 263-274 in Insulation Materials: Testing and Applications, 2nd Volume, ASTM STP 1116, R. S. Graves and D. C. Wysocki, Eds., American Society for Testing and Materials, Philadelphia, 1991.

8. Anne Silberstein, Eric Arquis, and David J. McCaa, "Forced Convection Effects in Fibrous Thermal Insulation," pp. 292-309 in Insulation Materials: Testing and Applications, 2nd Volume, R. S. Graves and D. C. Wysocki, Eds., American Society for Testing and Materials, Philadelphia, 1991.

9. C. Langlais, E. Arquis, and D. J. McCaa, "A Theoretical and Experimental Study of Convective Effects in Loose-Fill Thermal Insulation," pp. 290-318 in Insulation Materials, Testing, and Applications, ASTM STP 1030, D. L. McElroy and J. F. Kimpflen, Eds., American Society for Testing and Materials, Philadelphia, 1990.

10. Anne Silberstein, Catherine Langlais, and Eric Arquis, "Natural Convection in Light Fibrous Insulating Materials with Permeable Interfaces: Onset Criteria and Its Effect on the Thermal Performances of the Product," pp. 22-42 in Journal of Thermal Insulation, Volume 14, July, 1990.

11. A. Delmas and K. E. Wilkes, "Numerical Analysis of Heat Transfer by Conduction and Natural Convection in Loose-Fill Insulation-Effects of Convection on Thermal Performance," ORNL/CON-338, Oak Ridge National Laboratory, Oak Ridge, TN, 1992.

12. D. A. Nield and A. Bejan, Convection in Porous Media New York: Springer-Verlag, 1992.

13. W. R. Huntley, Design description of the large scale climate simulator, ORNL/TM-10675. Oak Ridge National Laboratory, Oak Ridge, TN, 1989.

14. Unisul, Inc., P. O. Box 1310, Winter Haven, FL 33992-1310.

15. K. E. Wilkes and P. W. Childs, Thermal Performance of Fiberglass and Cellulose Attic

Insulations, pp. 357-367, in Thermal Performance of the Exterior Envelopes of Buildings V, Proceedings of the ASHRAE/DOE/BTECC Conference, December, 1992.

16. "Standard Test Method for Steady-State Thermal Transmission Properties by Means of the Thin-Heater Apparatus," ASTM C 1114-89, pp. 608-616, in 1992 Annual Book of ASTM Standards, Vol. 04.06, American Society for Testing and Materials, Philadelphia, 1992.

17. D. L. McElroy, R. S. Graves, D. W. Yarbrough, and J. P. Moore, "A Flat Insulation Tester that Uses an Unguarded Nichrome Screen Wire Heater," Guarded Hot Plate and Heat Flow Meter Methodology, pp.339-355, ASTM STP 879, Edited by C. J. Shirtliffe and R. P. Tye, American Society for Testing and Materials, Philadelphia, 1985.

18. R. S. Graves, D. W. Yarbrough, D. L. McElroy, "Apparent Thermal Conductivity Measurements by an Unguarded Technique," Thermal Conductivity 18, pp. 339-355, Edited by T. Ashworth and David R. Smith. Plenum Press, New York, 1985.

19. D. L. McElroy, R. S. Graves, D. W. Yarbrough, and F. J. Weaver, "Laboratory Test Results on the Thermal Resistance of Polyisocyanurate Foamboard Insulation Blown with CFC-ll Substitutes-A Cooperative Industry/Government Project," ORNL/TM-11645, September 1991.

20. "Standard Test Method For Air Flow Resistance of Acoustical Materials", ASTM C 522- 87, pp. 170-174 in 1992 Annual Book of ASTM Standards, Vol. 04.06, American Society for Testing and Materials, Philadelphia, 1992.

21. K. E. Wilkes and R. S. Graves, "Air-Flow Permeability of Attic Insulation Materials," ORNL/M-2646, Oak Ridge National Laboratory, Oak Ridge, Tennessee, September 1993.

22. ASHRAE Handbook of Fundamentals, Chapters 20 and 22, American Society of Heating, Refrigerating and Air-conditioning Engineers, Inc., Atlanta. GA 1993.

23. Y. S. Touloukian, et al., editors, *Thermophysical Properties of Matter*, IFI/Plenum, New York, 1970.

APPENDIX A
TABLE OF NOMENCLATURE

R(SS) is the surface-to-surface thermal resistance, $m^2 \cdot K/W$,

A is the effective area of the ceiling exposed to the metering chamber, 6.44 m^2,

T_b is the temperature of the bottom of the gypsum board, K or °C,

T_t is the temperature at the top of the insulation, K or °C,

Q is the heat flow, W,

k is the thermal conductivity, W/m·K,

I is the current, amperes,

ΔV is the voltage, volts,

L is the insulation thickness, m,

A_o is the screen meter area, 0.5575 m^2 (UTHA),

ΔT is the temperature difference between the screen and the plates, K,

V is the filtration velocity, m/s,

K is the air flow permeability, m^2,

μ is the dynamic viscosity of air, kg/m·s,

dP/dx is the pressure gradient through porous medium, Pa/m,

F is the volumetric flow rate, m^3/s,

A is the specimen area perpendicular to the flow, m^2,

L is the thickness of specimen in flow direction, m,

ΔP is the pressure difference across the specimen, Pa,

ρ is the density in kg/m^3,

g is the acceleration of gravity, m/s^2,

β is the volume expansion coefficient, K^{-1},

C_p is the specific heat, J/kg·K,

ν is the kinematic viscosity of air, m^2/s,

ΔT is the temperature difference across the porous medium.

INTERNAL DISTRIBUTION

1-2. Central Research Library
3. Document Reference Section
4-5. Laboratory Records Department
6. Laboratory Records, ORNL RC
7. ORNL Patent Section
8-10. M&C Records Office
11. R. S. Carlsmith
12. J. E. Christian
13. G. E. Courville
14. A. O. Desjarlais
15-19. R. S. Graves
20. T. G. Kollie
21-25. D. L. McElroy
26-30. L. M. Parker
31. K. E. Wilkes
32. D. W. Yarbrough

EXTERNAL DISTRIBUTION

33. Albers, Mark, Schuller International, Mountain Technical Center, P. O. Box 625005, Littleton, CO 80162-5005
34. Bankvall, C., SP, P. O. Box 857, S-50115, Boras, Sweden
35. Delmas, A., 3 bis Ave Dulrievoz, 69100 Villeurbanne, France
36. Edmunds, W.M., Owens-Corning Fiberglas, 2790 Columbus Road, Route 16, Granville, OH 43023
37. Fellinger, Tom, Schuller International, Mountain Technical Center, P. O. Box 625005, Littleton, CO 80162-5005
38. Gilbo, C. F., 1820 Westcott Drive, Lancaster, PA 17603
39. Howerton, K., Federal Trade Commission, (Room S-4631) Sixth and Pennsylvania Avenue, NW, Washington, D.C. 20580
40. Langlais, C., Isover Saint Gobain, Centre de Recherches Industrelles, BP 19, 60290, Rantigny, France
41. McCaa, D. J., Certainteed Corporation, 1400 Union Meeting Road, Blue Bell, PA 19422
42. Mumaw, J. R., Owens-Corning Fiberglas, 2790 Columbus Road, Route 16, Granville, OH 43023
43. Nelson, Bruce, Minnesota Department of Public Service, 121 7th Pl E #200, St. Paul, MN 55101-2115
44. Ray, Richard, Schuller International, Mountain Technical Center, P. O. Box 625005, Littleton, CO 80162-5005
45. Rose, W., University of Illinois at Urbana-Champaign, One East Saint Mary's Road, Champaign, IL 61820
46. Scofield, M. P., Department of Energy, CE 421 FORSTL, 1000 Independence Avenue, Washington, D. C. 20585
47. Tong, T. W., Arizona State University, Department of Mechanical Engineering, Box 876106, Tempe, AZ 85287-6106
48. Tuluca, A., Steven Winter Associates, 50 Washington Street, Norwalk, CT 06859

49-50. Office of Scientific and Technical Information, P. O. Box 62, Oak Ridge, TN 37831

51. Office of Assistant Manager and Energy Research and Development, DOE-ORO, P. O. Box 2008, Oak Ridge, TN 37831-6269